Exact solutions of the nonlinear space-time fractional Schamel equation

Elzain A. E. Gumma [1], *, Abaker A. Hassaballa [1], Fathea M. O. Birkea [1], Ahmed M. A. Adam [1], Ali Satty [1], Emad A. B. Abdel-Salam [2], Eltayeb A. Yousif [3], Mohamed I. Nouh [4]

[1]Department of Mathematics, College of Science, Northern Border University, Arar, Saudi Arabia
[2]Department of Mathematics, Faculty of Science, New Valley University, Elkharga, Egypt
[3]Department of Applied Mathematics, Faculty of Mathematical Sciences and Informatics, University of Khartoum, Khartoum, Sudan
[4]Astronomy Department, National Research Institute of Astronomy and Geophysics (NRIAG), Cairo, Egypt

A B S T R A C T

This study focuses on the nonlinear space-time behavior of a plasma system made up of electrons, positive ions, and negative ions using the fractional Schamel (FS) equation. The main goal is to find exact solutions to the nonlinear FS equation by applying the extended hyperbolic function (EHF) method. The study examines how the fractional order affects the phase velocity, amplitude, and wave width of solitary wave solutions. Different exact solutions were found based on various values of the fractional order. Graphical representations are included to show the physical properties of these solutions. Overall, the results demonstrate that the EHF method is effective and reliable for finding exact solutions to the nonlinear FS equation.

1. Introduction

The nonlinear complicated physical phenomena associated with nonlinear partial differential equations (NLPDEs) have become increasingly important in a wide range of disciplines, including engineering, chemistry, biology, and plasma physics, making the search for exact solutions to these equations crucial. Since NLPDEs are mathematical representations of phenomena, studying their exact solutions might aid in understanding the underlying process of these physical models or improve understanding of the physical issue and its potential applications. With this goal in mind, a wide range of effective and straightforward techniques for determining the precise significant solutions of the NLPDEs despite their relative difficulty have been developed. Notable among these is Hirota's direct method (Hirota, 2004), which offers a systematic approach to constructing multi-soliton solutions. The F-expansion technique (Xue-Qin and Hong-Yan, 2008) provides a framework for generating a wide class of exact solutions. Additionally, the tanh-function method and its extended version (Wazwaz,

2010) are widely recognized for their efficacy in deriving solitary wave solutions. Other significant contributions to this domain are detailed in references (El-Ajou et al., 2019; Hassan, 2010; Sirendaoreji, 2007), collectively enriching the analytical tools available for exploring NLPDEs.

Plasma wave propagation is one of the most important subjects in plasma physics (Cho, 1990; Scales and Bernhardt, 1991). The nonlinear waves in plasma can be described by a variety of NPDEs, including the Korteweg-de-Vries-like (KdV) equation and the nonlinear Schrodinger-type (NLS) equations (Hietarinta, 1987; Zhong et al., 2023). Numerous researchers have conducted extensive studies on the propagation of waves, both linear and nonlinear, through a plasma system comprised of electrons, positive ions, and negative ions (Cho, 1990; Scales and Bernhardt, 1991). The study of wave propagation in plasmas with relativistic velocities, particularly when considering the presence of streaming ions, has yielded intriguing results (Ghosh et al., 2008; Hafez et al., 2016). These results have revealed that relativistic effects significantly influence the formation of ion-acoustic solitons, a phenomenon that becomes pronounced solely in conjunction with ion streaming.

The Schamel equation (Schamel, 1973) is a modified form of the Korteweg-de Vries (KdV) equation that includes terms to model the effects of trapped particles in a plasma, which can influence the properties of solitons and other nonlinear structures. When we refer to a fractional Schamel

(FS) equation, we're likely discussing an adaptation that involves fractional derivatives, which allows for a more accurate description of anomalous diffusion or other complex processes that are not adequately captured by integer-order calculus. The emphasis of this study is to find exact wave solutions for the FS equation by utilizing the conformable fractional derivative (CFD) approach. Introduced by Khalil et al. (2014), CFD represents a significant advancement in fractional calculus, providing a derivative with distinctive properties that find extensive applications across various fields, notably including mathematics, engineering, and physics. The application of CFD in soliton theory is distinctly beneficial for its capability to elucidate the dynamics of soliton waves and to yield a deep understanding of the underlying physical phenomena. Bearing these advantages in consideration, the current study employs the EHF method to extract traveling wave solutions pertaining to the FS equation.

The EHF method (Shang, 2008) stands as a significant method for obtaining traveling wave solutions for various NPDEs. The exploration of its applicability to the FS equation, however, is an area that has not been thoroughly investigated. The novelty of this study is attributed to the application of the EHF method to the FS equation—a technique seldom employed for this specific equation. This not only aims to augment the collection of exact solutions for the FS equation but also seeks to provide a more profound understanding of the intricate dynamics characteristic of fractional-order nonlinear systems. A variety of studies have employed this method to investigate diverse NPDEs, aiming to acquire traveling wave solutions, see for example (Rehman et al., 2022; Rezazadeh et al.,2021; Karakoç et al., 2023).

This paper demonstrates the derivation of solitary wave solutions in plasmas encompassing negative ions, positive ions, and electrons. The Schamel equations are deduced by employing the EHF method on the fundamental equations, with particular consideration given to the influences of negative ions, positive ions, and electron dynamics. The main objective of this study is to acquire the exact solutions of the nonlinear fractional FS equation. The organization of this paper is structured as follows: Section 2 provides the properties of the CFD, derived fundamental model, and application of the EHF method. This section also presents the obtained solutions for the FS equation. In Section 3, graphical depictions are employed to elucidate the physical attributes of the solutions derived. The paper culminates with concluding remarks and future research directions in Section 4.

2. Methodology

2.1. CFD

In this subsection, we present a concise discussion of the fundamental properties of CFD, following the monographs authored by Khalil et al.

(2014). We define the conformable derivative of order α, where $0 < \alpha \leq 1$, with respect to the independent variable x as:

$$D^\alpha M(s) = \lim_{h \to 0} \frac{M(s + hs^{1-\alpha}) - M(s)}{h}, \forall s > 0, \alpha \in (0,1],$$
$$M^{(\alpha)}(0) = \lim_{s \to 0^+} M^{(\alpha)}(s). \tag{1}$$

Putting $\alpha = 1$ in the last equation, the non-integer differential becomes the well-known integer differential. The CFD satisfied the following axioms:

- $D^\alpha s^n = ns^{n-\alpha}, n \in R,$
- $D^\alpha a = 0,$
- $D^\alpha(aM + bN) = aD^\alpha M + bD^\alpha N, \forall a, b \in R,$
- $D^\alpha(MN) = MD^\alpha N + ND^\alpha M,$
- $D^\alpha\left(\frac{M}{N}\right) = \frac{MD^\alpha N - ND^\alpha M}{N^2},$
- $D^\alpha M(N) = \frac{dM}{dN}D^\alpha N, D^\alpha M(s) = s^{1-\alpha}\frac{dM}{ds},$

where, M, N are two α−differentiable functions of a dependent variable s, and a is constant. These properties have been well-proven and share many properties with integer derivatives (Khalil et al., 2014). It is noted that the conformable differential operator complies with several fundamental principles analogous to those of the chain rule, Taylor series expansion, and Laplace transformation (Abdeljawad, 2015). In this paper, the FKP equation is translated into an ODE within the context of CFD.

2.2. Deriving the fundamental model

The foundational equations presented herein characterize the propagation dynamics of theoretical ion acoustic waves within a cold, non-collisional plasma comprised of both positively and negatively charged ions, as framed by the concept of CFDs. It is posited that the positively charged ions are,

$$D_t^\alpha n_i + D_x^\alpha(n_i v_i) = 0, \tag{2}$$
$$D_t^\alpha v_i + v_i D_x^\alpha v_i = -D_x^\alpha \varphi, \tag{3}$$

and negatively charged ions are,

$$D_t^\alpha n_j + D_x^\alpha(n_j v_j) = 0, \tag{4}$$
$$D_t^\alpha v_j + v_j D_x^\alpha v_j = R^{-1}D_x^\alpha \varphi. \tag{5}$$

Fractional Poisson's equation is,

$$D_x^{\alpha\alpha}\varphi = n_e + n_j - n_i. \tag{6}$$

In the provided notation, the subscripts i and j are assigned to positive and negative ions, respectively, while the subscript e is designated for electrons. The term R is defined as the mass ratio $\frac{m_j}{m_i}$, which quantifies the relative mass of a negative ion to that of a positive ion. Normalization is applied to physical quantities that exist in these equations: n_i, n_j and n_e are the densities via equilibrium density electron n_0, φ is the potential electrostatic, v is the velocity of the ion flow in the x direction, n_e is the electron density of charge particles, n_i for positive ions and n_j for negative ions and D_x^α is the

conformable fractional differential with respect to x, $D_x^{\alpha\alpha} = D_x^\alpha D_x^\alpha$ is the twice conformable fractional differential with respect to x. Assuming that low-frequency ion acoustic waves and electrons are in quasi-equilibrium $n_e \simeq n_i - n_j$, and $n_e(\varphi)$ for the two cases $\beta > 0$ and $\beta < 0$ has the formula (El-Kalaawy, 2011),

$$n_e(\varphi) = 1 + \varphi - \frac{4}{3\sqrt{\pi}}(1-\beta)\varphi^{\frac{3}{2}} + \frac{1}{2}\varphi^2. \tag{7}$$

Through the application of reductive perturbation techniques, the scale's new stretching coordinates (time and space) are provided as,

$$\xi = \frac{\sqrt[4]{\varepsilon}}{\alpha}(x^\alpha - \alpha v_0 t^\alpha), \tau = \frac{\sqrt[4]{\varepsilon^3}t^\alpha}{\alpha}, \tag{8}$$

where, ε represents a diminutive parameter that signifies the degree of dispersion. The phase velocity within the (x,t) coordinate system, denoted as v_0, remains an undetermined variable which requires determination. Within the context of a quasi-equilibrium plasma state, this phase velocity is standardized to one. To proceed, we perform expansions for the particle densities n_i and n_j, the velocities v_i and v_j, as well as the electric potential φ, in terms of powers of the small parameter ε, adhering closely to conditions associated with the quasi-equilibrium state. Thus,

$$
\begin{aligned}
n_i &= n_{i0} + \varepsilon n_{i1} + \varepsilon^{\frac{3}{2}} n_{i2} + \cdots, \\
n_j &= n_{j0} + \varepsilon n_{j1} + \varepsilon^{\frac{3}{2}} n_{j2} + \cdots, \\
v_i &= \varepsilon v_{i1} + \varepsilon^{\frac{3}{2}} v_{i2} + \cdots, \\
v_j &= \varepsilon v_{j1} + \varepsilon^{\frac{3}{2}} v_{j2} + \cdots, \\
\varphi &= \varepsilon \varphi_1 + \varepsilon^{\frac{3}{2}} \varphi_2 + \cdots.
\end{aligned}
\tag{9}
$$

By applying reductive perturbation expansion to the aforementioned set of equations, the following coupled equations are acquired,

$$-\alpha v_0 D_\xi^\alpha n_{i1} + n_{i0} D_\xi^\alpha v_{i1} = 0, \tag{10a}$$
$$-\alpha v_0 D_\xi^\alpha n_{j1} + n_{j0} D_\xi^\alpha v_{j1} = 0, \tag{10b}$$
$$-\alpha v_0 D_\xi^\alpha n_{i2} + D_\tau^\alpha n_{i1} + n_{i0} D_\xi^\alpha v_{i2} = 0, \tag{10c}$$
$$-\alpha v_0 D_\xi^\alpha n_{j2} + D_\tau^\alpha n_{j1} + n_{j0} D_\xi^\alpha v_{j2} = 0, \tag{10d}$$
$$-\alpha v_0 D_\xi^\alpha v_{i1} + D_\xi^\alpha \varphi_1 = 0, \tag{10e}$$
$$-\alpha v_0 D_\xi^\alpha v_{j1} - \frac{1}{R} D_\xi^\alpha \varphi_1 = 0, \tag{10f}$$
$$-\alpha v_0 D_\xi^\alpha v_{i2} + D_\tau^\alpha v_{i1} + D_\xi^\alpha \varphi_2 = 0, \tag{10g}$$
$$-\alpha v_0 D_\xi^\alpha v_{j2} + D_\tau^\alpha v_{j1} - \frac{1}{R} D_\xi^\alpha \varphi_2 = 0, \tag{10h}$$
$$n_{i0} - n_{j0} = 1, n_{j1} - n_{i1} + \varphi_1 = 0, \tag{10i}$$
$$D_\xi^{\alpha\alpha} \varphi_1 = n_{j2} - n_{i2} + \varphi_2 + \frac{4(\beta-1)}{3\sqrt{\pi}}\varphi_1^{\frac{3}{2}}. \tag{10j}$$

From the above equations, we can obtain,

$$
\begin{aligned}
n_{i1} &= \frac{n_{i0}}{\alpha^2 v_0^2}\varphi_1, n_{j1} = -\frac{n_{i0}}{R\alpha^2 v_0^2}\varphi_1, \\
v_{i1} &= \frac{1}{\alpha^2 v_0^2}\varphi_1, v_{j1} = -\frac{1}{R\alpha^2 v_0^2}\varphi_1,
\end{aligned}
\tag{11}
$$

under the boundary conditions,

(i) $n_{i1} = v_{i1}, n_{j1} = v_{j1}, at\ |\xi| \to \infty,$
(ii) $\varphi_1 = 0,$ (12)

then, we obtain $\frac{n_{i0}}{\alpha^2 v_0^2} + \frac{n_{j0}}{R\alpha^2 v_0^2} = 1$, and therefore, the phase velocity v_0 can be given by,

$$\alpha^2 v_0^2 = n_{i0} + \frac{n_{j0}}{R}. \tag{13}$$

Eliminating $n_{i2}, v_{i2}, n_{j2}, v_{j2}, \varphi_2$ and using Eq. 10h, for ion acoustic waves, we derive the following nonlinear FS equation,

$$D_\tau^\alpha \varphi + \frac{\alpha v_0(1-\beta)}{\sqrt{\pi}}\varphi^{\frac{1}{2}} D_\xi^\alpha \varphi + \frac{\alpha v_0}{2} D_\xi^{\alpha\alpha\alpha}\varphi = 0. \tag{14}$$

2.3. Application of the extended hyperbolic function (EHF) method

Consider an NPDE for $\varphi(\xi, \tau)$ in the form,

$$P(\varphi, D_\tau^\alpha \varphi, D_\xi^\alpha \varphi, D_{\xi\xi}^{\alpha\alpha}\varphi, D_{\tau\xi}^{\alpha\alpha}\varphi, \dots) = 0. \tag{15}$$

Introducing the similarity variable $\zeta = k(\xi^\alpha - u_0\tau^\alpha)/\alpha$, where u_0 is a steady speed, the wave number is k, hence the next ordinary differential equation (ODE) is satisfied by the function $\varphi(\xi)$,

$$F(\varphi, \varphi_\zeta, \varphi_{\zeta\zeta}, \varphi_{\zeta\zeta\zeta}, \dots) = 0. \tag{16}$$

We suppose that the following to be the solution to Eq. 15,

$$
\begin{aligned}
\varphi(\zeta) &= a_0 + \sum_{i=1}^N \left[a_i g^i(\zeta) + b_i g^{-i}(\zeta)\right] + \\
&\quad \sum_{i=2}^N c_i g^{i-2}(\zeta)g'(\zeta) + \sum_{i=1}^N d_{-i} g^{-i}(\zeta)g'(\zeta),
\end{aligned}
\tag{17}
$$

where, the constants a_0, a_i, b_i, c_i, and d_i require determination, and where N represents a positive integer. To ascertain the appropriate value for the positive integer N, one employs the method of homogeneous balance between the dominating nonlinear terms and the superior derivatives of the function $\varphi(\zeta)$ as delineated in Eq. 16. Additionally, the function $g(\zeta)$ is indicative of the following solutions to the accompanying auxiliary ODEs.

$$
\begin{aligned}
\frac{dg}{d\zeta} &= g\sqrt{A + Bg^2}, \frac{d^2g}{d\zeta^2} = Ag + 2Bg^3, \\
\frac{d^3g}{d\zeta^3} &= g(A + 6Bg^2)\sqrt{A + Bg^2},
\end{aligned}
\tag{18}
$$

where, A and B are actual parameters that will be chosen based on $g(\zeta)$. By extending the mapping discussed earlier, we derive additional solutions. Incorporating Eq. 17 into Eq. 16, and integrating Eq. 18, we can transform the left-hand side of Eq. 16 into a polynomial in terms of $g^m(\zeta)$, where m encompasses both negative and positive integers, including zero. The process of equating to zero the coefficients corresponding to each power of $g^m(\zeta)$ results in a suite of algebraic equations for the parameters k, a_0, a_i, b_i, c_i and d_i. Utilizing software such as Maple facilitates solving these equations and allows us to express k, a_0, a_i, b_i, c_i and d_i in terms of constants q_0, q_2, and q_4. Subsequently integrating these findings back into Eq. 17 and employing the previously defined mapping leads to the derivation of periodic wave solutions for Eq. 16.

In Eq. 14, if we set $\varphi(\xi,\tau) = u^2(\xi,\tau)$, we obtain,

$$2uD_\tau^\alpha u + 2au^2 D_\xi^\alpha u + \alpha v_0 u D_\xi^{\alpha\alpha\alpha} u + 3\alpha v_0 D_\xi^\alpha u D_\xi^{\alpha\alpha} u = 0, \quad (19)$$

with $a = \frac{\alpha v_0(1-\beta)}{\sqrt{\pi}}$, and through replacing,

$$u(\xi,\tau) = \psi(\zeta), \zeta = k(\xi^\alpha - u_0\tau^\alpha)/\alpha, \quad (20)$$

into Eq. 19, after performing a single integration with respect to ζ and setting the integration constant to zero, we obtain,

$$-u_0\psi^2 + \alpha v_0 k^2\left[\left(\frac{d\psi}{d\zeta}\right)^2 + \psi\frac{d^2\psi}{d\zeta^2}\right] + \frac{2a}{3}\psi^3 = 0, \quad (21)$$

taking the answer when ψ^3 and $\psi\frac{d^2\psi}{d\zeta^2}$ are balanced since it yields the leading order, $N = 2$.

$$\psi(\zeta) = a_0 + a_1 g(\zeta) + a_2 g^2(\zeta) + \frac{b_1}{g(\zeta)} + \frac{b_2}{g^2(\zeta)} + c_2 g'(\zeta) + \frac{d_1 g'(\zeta)}{g(\zeta)} + \frac{d_2 g'(\zeta)}{g^2(\zeta)}, \quad (22)$$

where, $g(\zeta)$ is the solution to Eq. 18, $a_0, a_1, a_2, b_1, b_2, c_2, d_1, d_2$ and k are constants that must be founded. Eq. 18 and Eq. 22 are substituted into Eq. 21 with the coefficients of $g^m(\zeta)$ set to zero. This result is a system of nonlinear algebraic equations for $a_0, a_1, a_2, b_1, b_2, c_2, d_1, d_2$ and k, which can be solved using Maple, we have:

• Case 1:

$$a_2 = -\frac{15Bu_0}{8a\alpha Av_0}, k = \pm\sqrt{\frac{u_0}{8\alpha Av_0}}, a_0 = a_1 = b_1 = b_2 = c_2 = d_1 = d_2 = 0. \quad (23)$$

• Case 2:

$$a_0 = \frac{15u_0}{22a}, k = \pm\sqrt{\frac{2u_0}{11A\alpha v_0}}, b_2 = \frac{15u_0 A}{44aB},$$
$$d_2 = -\frac{15u_0}{22a\sqrt{B}}, a_1 = a_2 = b_1 = c_2 = d_1 = 0. \quad (24)$$

$$\varphi(\zeta) = \left[a_0 + \frac{b_2}{g^2(\zeta)} + \frac{d_2 g'(\zeta)}{g^2(\zeta)}\right]^2 = \left[\frac{15u_0}{22a} + \frac{15u_0 A}{44aB g^2(\zeta)} - \frac{15u_0 g'(\zeta)}{22a\sqrt{B} g^2(\zeta)}\right]^2,$$
$$\zeta = \pm\sqrt{\frac{2u_0}{11\alpha\ Av_0}}(\xi^\alpha - u_0\tau^\alpha) + \theta. \quad (31)$$

1. If $A > 0, B > 0$, then we obtain:

$$\varphi_5(\zeta) = \left[\frac{15u_0}{22a} + \frac{15u_0}{44a\mathrm{csch}^2(\sqrt{A}\zeta)} + \frac{15u_0\coth(\sqrt{A}\zeta)}{22a\mathrm{csch}(\sqrt{A}\zeta)}\right]^2. \quad (32)$$

2. If $A < 0, B > 0$, then we obtain:

$$\varphi_6(\zeta) = \left[\frac{15u_0}{22a} + \frac{15u_0}{44a\sec^2(\sqrt{-A}\zeta)} - \frac{15u_0\tan(\sqrt{-A}\zeta)}{22a\sec(\sqrt{-A}\zeta)}\right]^2. \quad (33)$$

• Case 3:

$$a_0 = \frac{9u_0 A^2}{8a}, k = \pm\sqrt{\frac{-u_0 A^3}{10\alpha v_0}}, a_2 = \frac{3u_0 AB}{2a},$$
$$b_2 = -\frac{3A^3 u_0}{16aB}, a_1 = b_1 = c_2 = d_1 = d_2 = 0. \quad (25)$$

Family 1: Substituting Eq. 23 into Eq. 22, we derive the subsequent concentration formulas for traveling wave solutions of Eq. 14 as:

$$\varphi(\zeta) = [a_2 g^2(\zeta)]^2 = \left[\frac{15Bu_0}{8a\alpha Av_0}g^2(\zeta)\right]^2, \zeta = \pm\sqrt{\frac{u_0}{8\alpha^4 Av_0}}(\xi^\alpha - u_0\tau^\alpha) + \theta, \quad (26)$$

where, the parameter θ is the phase shift.

1. If $A > 0, B > 0$, then we can obtain:

$$\varphi_1(\zeta) = \left[\frac{15u_0}{8a\alpha v_0}\mathrm{csch}^2(\sqrt{A}\zeta)\right]^2, \zeta = \pm\sqrt{\frac{u_0}{8\alpha^4 Av_0}}(\xi^\alpha - u_0\tau^\alpha) + \theta. \quad (27)$$

2. If $A < 0, B > 0$, then we can obtain:

$$\varphi_2(\zeta) = \left[\frac{15u_0}{8a\alpha v_0}\sec^2(\sqrt{-A}\zeta)\right]^2, \zeta = \pm\sqrt{\frac{u_0}{8\alpha^4 |A|v_0}}(\xi^\alpha - u_0\tau^\alpha) + \theta. \quad (28)$$

$$\varphi_3(\zeta) = \left[\frac{15u_0}{8a\alpha v_0}\csc^2(\sqrt{-A}\zeta)\right]^2, \zeta = \pm\sqrt{\frac{u_0}{8\alpha^4 |A|v_0}}(\xi^\alpha - u_0\tau^\alpha) + \theta. \quad (29)$$

3. If $A > 0, B < 0$, then we can obtain:

$$\varphi_4(\zeta) = \left[\frac{15u_0}{8a\alpha\ v_0}\mathrm{sech}^2(\sqrt{A}\zeta)\right]^2, \zeta = \pm\sqrt{\frac{u_0}{8\alpha^3 Av_0}}(\xi^\alpha - u_0\tau^\alpha) + \theta. \quad (30)$$

Family 2: Substituting Eq. 24 into Eq. 22, we derive the subsequent concentration formulas for traveling wave solutions of Eq. 14 as:

$$\varphi_7(\zeta) = \left[\frac{15u_0}{22a} + \frac{15u_0}{44a\csc^2(\sqrt{-A}\zeta)} + \frac{15u_0\cot(\sqrt{-A}\zeta)}{22a\csc(\sqrt{-A}\zeta)}\right]^2. \quad (34)$$

3. If $A > 0, B < 0$, then we obtain:

$$\varphi_8(\zeta) = \left[\frac{15u_0}{22a} + \frac{15u_0}{44a\mathrm{sech}^2(\sqrt{A}\zeta)} + \frac{15u_0\tanh(\sqrt{A}\zeta)}{22a\mathrm{sech}(\sqrt{A}\zeta)}\right]^2. \quad (35)$$

Family 3: Substituting Eq. 25 into Eq. 22, we derive the subsequent concentration formulas for traveling wave solutions of Eq. 14 as:

$$\varphi(\zeta) = \left[a_0 + a_2 g^2(\zeta) + \frac{b_2}{g^2(\zeta)}\right]^2 = \left[\frac{9u_0 A^2}{8a} + \frac{3u_0 AB}{2a}g^2(\zeta) - \frac{3A^3 u_0}{16aB}\frac{1}{g^2(\zeta)}\right]^2,$$
$$\zeta = \pm\sqrt{\frac{-u_0 A^3}{10\alpha^3 v_0}}(\xi^\alpha - u_0\tau^\alpha). \quad (36)$$

1. If $A > 0, B > 0$, then we obtain:

$$\varphi_9(\zeta) = \left[\frac{9u_0 A^2}{8a} + \frac{3u_0 A^2}{2a}\operatorname{csch}^2(\sqrt{A}\zeta) - \frac{3A^2 u_0}{16a}\frac{1}{\operatorname{csch}^2(\sqrt{A}\zeta)}\right]^2. \quad (37)$$

2. If $A < 0, B > 0$, then we obtain:

$$\varphi_{10}(\zeta) = \left[\frac{9u_0 A^2}{8a} + \frac{3u_0 A^2}{2a}\sec^2(\sqrt{-A}\zeta) - \frac{3A^2 u_0}{16a}\frac{1}{\sec^2(\sqrt{-A}\zeta)}\right]^2. \quad (38)$$

$$\varphi_{11}(\zeta) = \left[\frac{9u_0 A^2}{8a} + \frac{3u_0 A^2}{2a}\csc^2(\sqrt{-A}\zeta) - \frac{3A^2 u_0}{16a}\frac{1}{csc^2(\sqrt{-A}\zeta)}\right]^2. \quad (39)$$

3. If $A > 0, B < 0$, then we obtain:

$$\varphi_{12}(\zeta) = \left[\frac{9u_0 A^2}{8a} + \frac{3u_0 A^2}{2a}\operatorname{sech}^2(\sqrt{A}\zeta) - \frac{3A^2 u_0}{16a}\frac{1}{\operatorname{sech}^2(\sqrt{A}\zeta)}\right]^2. \quad (40)$$

From solution of Eq. 30, the quantity $A_m = \frac{225\pi u_0^2}{64\alpha^4(1-\beta)^2 v_0^4}$ represent the wave amplitude and $W = \sqrt{\frac{8\alpha^4 v_0}{u_0}}$ represent the wave width depending on the fractional order α. It should be highlighted in this solution that the perturbation method is not applicable for large propagation and is only suitable for small but finite amplitude limits. There are isolated waves with only positive potential as $u_0 > 0$. Empirical observations indicate that an increase in the initial condition u_0 correlates with a reduction in width and an augmentation in amplitude. Conversely, a rise in the absolute value of β is associated with a diminution of amplitude when β is less than zero and an enhancement when β is greater than zero. Additionally, the FS equation's stationary solitary solution is,

$$\frac{2}{\alpha v_0}D_\tau^\alpha \varphi + \frac{4(-1+\beta)}{3\sqrt{\pi}}D_\xi^\alpha \varphi^{\frac{3}{2}} + D_\xi^{\alpha\alpha}\varphi = 0, \quad (41)$$

where, $a = \frac{4(-1+\beta)}{3\sqrt{\pi}}$ is the result of applying the proper boundary condition, namely $\varphi \to 0, D_\zeta^\alpha \varphi \to 0$ and $D_\zeta^{\alpha\alpha}\varphi \to 0$ as $|\chi| \to \infty$, and assuming the single variable $\chi = \zeta - u_0\tau^\alpha/\alpha$ concerning the propagating velocity u_0, which stands for the solitary wave speed. From the FS equation, the following fractional Sagdeev potential is obtained as:

$$-\frac{2u_0}{\alpha v_0}\varphi' + a\left(\varphi^{\frac{3}{2}}\right)' + \varphi''' = 0. \quad (42)$$

Upon integration of the preceding equation twice in accordance with the stipulated conditions, it is observed that the resulting constant of integration is zero, thereby confirming that Eq. 42 represents the definitive form. Therefore,

$$-V(\varphi) = \frac{u_0}{\alpha v_0}\varphi^2 - \frac{2a}{5}\varphi^{\frac{5}{2}}, \quad (43)$$

where, the pseudo-potential $V(\varphi)$ for our purposes reads,

$$\frac{1}{2}\left(\varphi_\chi\right)^2 = -V(\varphi). \quad (44)$$

An analysis of Eq. 43 reveals that the condition $(\varphi) = \frac{dV(\varphi)}{d\varphi} = 0$ is satisfied at $\varphi = 0$. Consequently, for Eq. 43 to admit solitary wave solutions, it is required that $V(\varphi)$ be less than zero in the interval $0 < \varphi < \phi$ and that $V(\phi)$ equals zero when $\varphi = \phi$, with ϕ representing the amplitude of the solitary waves. The fulfillment of the initial criterion necessitates that $(\frac{d^2V}{d\varphi^2})_{\varphi=0} < 0$ be negative. The other requirement, $V(\phi) = 0$, yields a relationship between the amplitude ϕ and the speed u_0 of the solitary wave, delineating what is known as the nonlinear dispersion relation. This facilitates deriving a solution for Eq. 43.

$$\varphi(\xi,\tau) = \frac{25u_0^2}{4\alpha^2 v_0^2 a^2}\operatorname{sech}^4\left(\sqrt{\frac{u_0}{\alpha^4 v_0}}(\zeta - u_0\tau^\alpha)\right), \quad (45)$$

where, $\frac{25u_0^2}{4\alpha^2 v_0^2 a^2}$ is the amplitude and $\sqrt{\frac{\alpha^4 v_0}{u_0}}$ is the width which are depending on the fractional order α.

Upon examining the findings acquired in this research and comparing them with prior studies, it can be observed that when the fractional order is equal to one, equations 1 through 13 correspond to the same equations as those derived by El-Kalaawy (2011). It is important to recognize that the solutions in the sequence from 26 to 40 correspond to those identified by El-Kalaawy (2011) when the conditions for the fractional order are set to one, and the parameters $\alpha = 1, q_0 = 0, q_2 = A, q_4 = B$ are applied. Furthermore, it is noted that upon setting the fractional order to unity, Eq. 45 yields a solution that coincides with the results previously reported by Williams et al. (2014).

3. Graphical representations

In this section, the nature of nonlinear FS equation created from Eq. 14 is visualized in the 3D graphs. In addition, their physically interpretation is also discussed.

In Fig. 1, the phase velocity v_0 of Eq. 13 is plotted via equilibrium density across varying values of the fractional order $\alpha = 1, 0.98, 0.96, 0.94, 0.92, 0.9$ at $R = 4$. Fig. 1A presents the phase velocity v_0 with respect to equilibrium density positive ions with $n_{j0} = 480000$. Fig. 1B represents the phase velocity v_0 with respect to equilibrium density negative ions with $n_{i0} = 4800000$. Fig. 1C is the 3D graph of the phase velocity v_0 via the equilibrium density positive and negative ions. Fig. 1 illustrates how the variations in equilibrium densities of both positively and negatively charged ions influence the phase velocity (v_0) within the spatiotemporal domain described by coordinates (x, t). For $\alpha = 1$, the increase of the n_{j0} and n_{i0} leads to increase of v_0. Decreasing the fractional order from 0.98 to 0.90 has been observed to enhance the phase velocity of the wave, illustrating that variations in the fractional order α are directly associated with alterations in wave propagation characteristics.
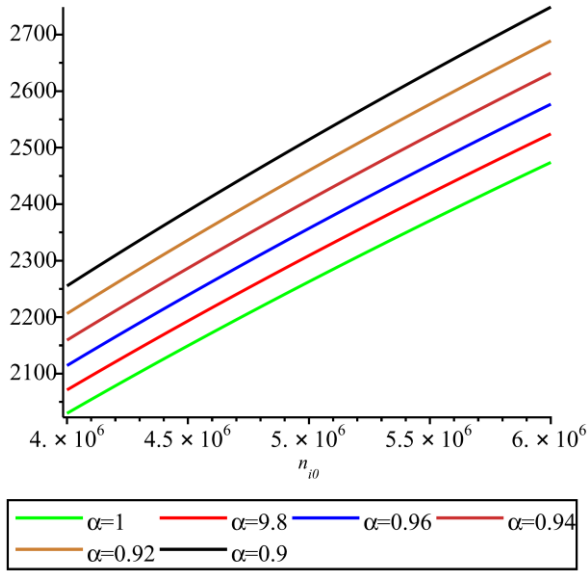
A: phase velocity v_0 with respect to equilibrium density positive ions with $n_{j0} = 480000$
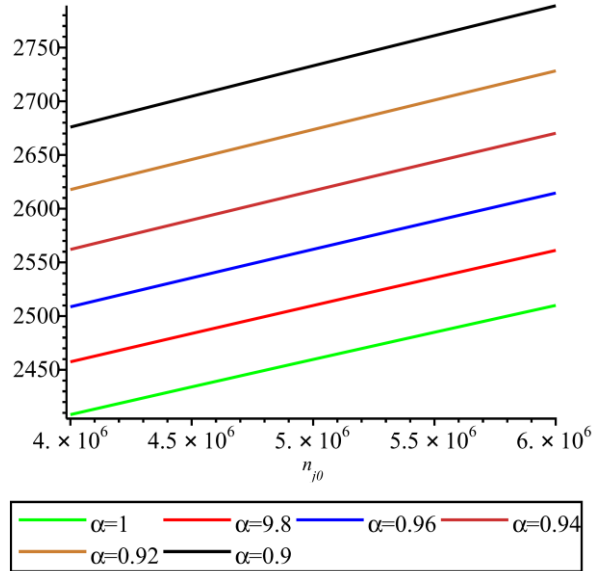
B: phase velocity v_0 with respect to equilibrium density negative ions with $n_{i0} = 4800000$
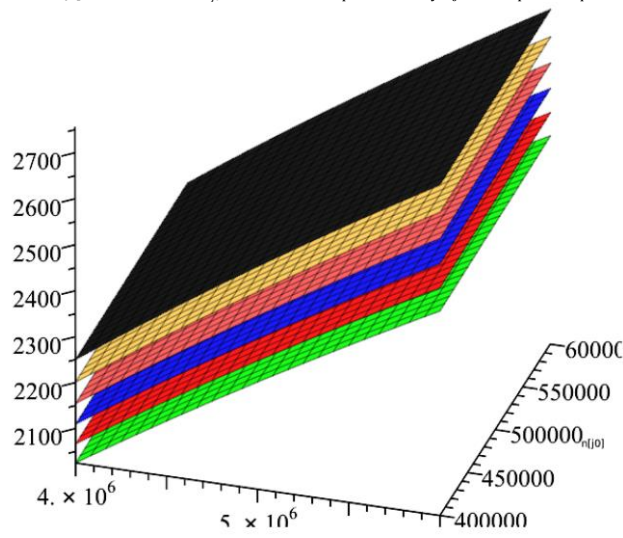
C: 3D graph of the phase velocity v_0 via the equilibrium density positive and negative ions

Fig. 1: The phase velocity v_0 versus the equilibrium density positive and negative ions with various fractional order, $\alpha = 1, 0.98, 0.96, 0.94, 0.92, 0.9$ at $R = 4$

Fig. 2 presents the wave amplitude A_m (presented after Eq. 40) when $\beta = -1.75$, with varied fractional order values, $\alpha = 1, 0.95, 0.9, 0.8, 0.7, 0.6$. In Fig. 2A the amplitude A_m is plotted versus v_0 when $u_0 = 0.25$. As shown in Fig. 2A the amplitude A_m decreases when v_0 varies from 1 to 2. The small value A_m when $\alpha = 1$ (green line).
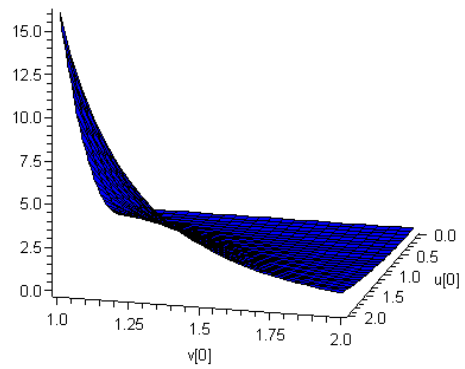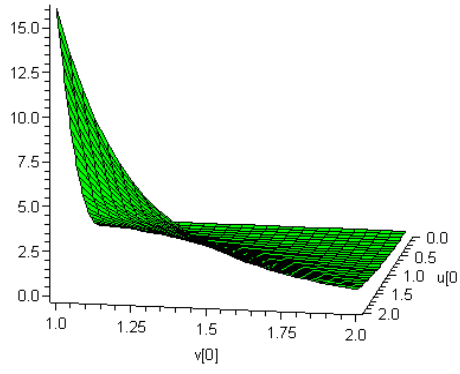
By decreasing the α from 0.95 to 0.6, we see that A_m increases. Fig. 2B presents the graph of wave amplitude A_m verses u_0 when $v_0 = 1.25$. Fig. 2C and Fig. 2D show 3D graphs for the wave amplitude A_m verses v_0 and u_0 with $\alpha = 1$ and $\alpha = 0.9$ respectively.
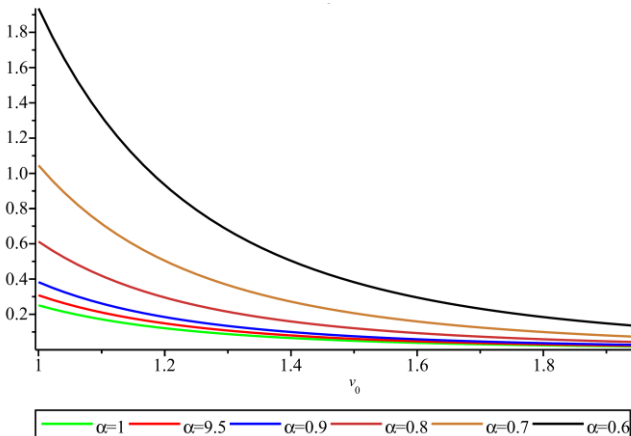
A: amplitude A_m is plotted versus v_0 when $u_0 = 0.25$
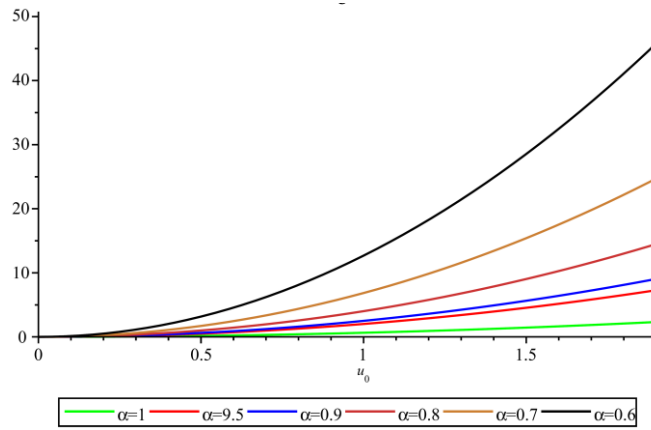
B: graph of wave amplitude A_m verses u_0 when $v_0 = 1.25$

C: 3D graphs for the wave amplitude A_m verses v_0 and u_0 with $\alpha = 1$ D: 3D graphs for the wave amplitude A_m verses v_0 and u_0 with $\alpha = 0.9$

Fig. 2: The amplitude A_m versus v_0 and u_0 with various fractional order $\alpha = 1, 0.95, 0.9, 0.8, 0.7, 0.6$ at $R = 4$
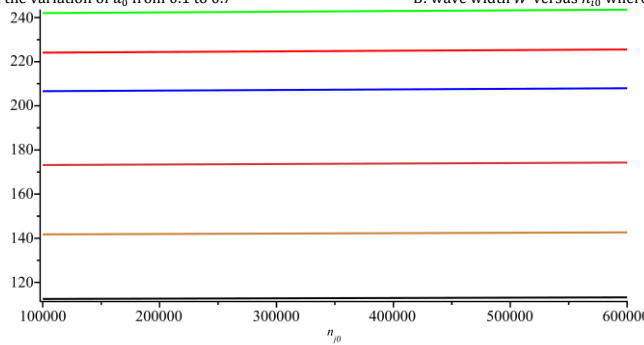
Fig. 3 represents the wave width W (presented after Eq. 40) versus u_0 when $n_{i0} = 4800000$, $n_{j0} = 480000$ and $R = 4$ across varied fractional order values, $\alpha = 1, 0.95, 0.9, 0.8, 0.7, 0.6$. As shown in Fig. 3A, the wave width W decreasing with the variation of u_0 from 0.1 to 0.7 and W begins from a greater value of $\alpha = 1$ (green line). By decreasing α from 0.95 to 0.6, we observe that W becomes smaller. Fig. 3B presents wave width W versus n_{i0}, where n_{i0} varies from 1000000 to 6000000 when $n_{j0} = 480000$, $u_0 = 0.3$ and $R = 4$ with different values of the fractional order $\alpha = 1, 0.95, 0.9, 0.8, 0.7, 0.6$. Fig. 3C presents wave width W versus n_{j0} where n_{j0} varies from 100000 to 600000 when $n_{i0} = 4800000$, $u_0 = 0.3$ and $R = 4$ different values of the fractional order $\alpha = 1, 0.95, 0.9, 0.8, 0.7, 0.6$. From Fig. 3, we deduce that wave width W decreasing by decreasing the fractional order α.
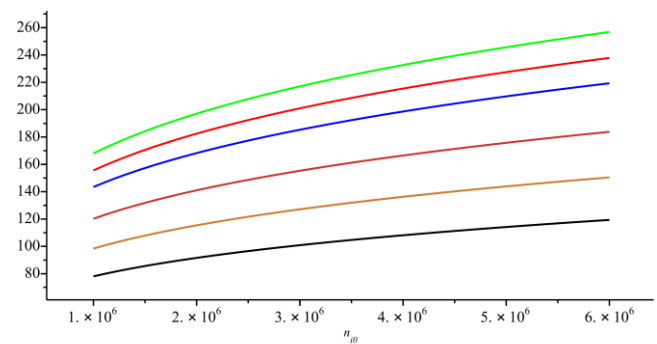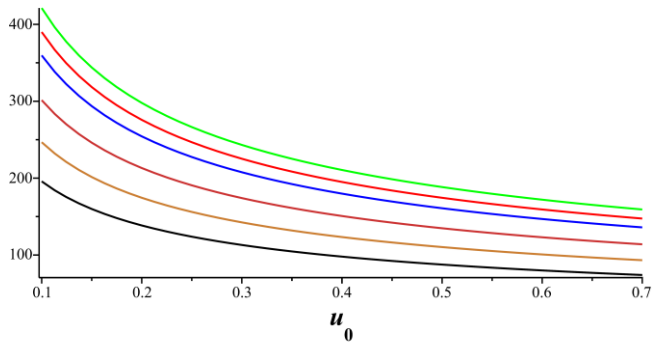
A: wave width W decreasing with the variation of u_0 from 0.1 to 0.7   B: wave width W versus n_{i0} where n_{i0} varies from 1000000 to 6000000

C: wave width W versus n_{j0} where n_{j0} varies from 100000 to 600000

Fig. 3: The wave width versus u_0 when $n_{i0} = 4800000$, $n_{j0} = 480000$ and $R = 4$

Fig. 4 represents the evolution behavior of soliton solution of Eq. 30 with $u_0 = 0.75$, $v_0 = 2.5, \beta = -1.75$, $a = 6.875/\sqrt{\pi}$. The green layer when $\alpha = 1$, the red layer when $\alpha = 0.95$ and the blue layer when $\alpha = 0.9$. We observe that the amplitude peak moves apart with the variation of fractional order. This means that the soliton solution depended on the fractional order.

4. Conclusion

This study investigated the complex non-linear space-time dynamics of a plasma system composed of a mixture of electrons, positive ions, and negative ions. This has been conducted within the context of the FS equation's framework. The EHF method was effectively employed to derive analytical solutions

for the FS equation, which incorporates the CFD. Detailed investigations have been conducted to elucidate the influence of the fractional order on properties such as phase velocity, amplitude, and wave width within the context of solitary wave solutions.
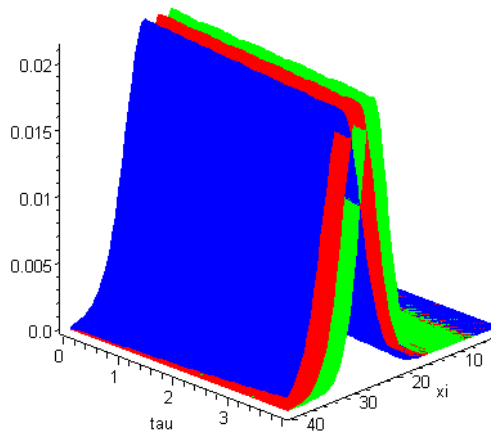

Fig. 4: Evolution behavior of soliton solution Eq. 30 with $u_0 = 0.75, v_0 = 2.5, \beta = -1.75$ with different values of $\alpha = 1,\ 0.95,\ 0.9$

A compendium of precise analytical solutions pertinent to the FS equation has been successfully delineated. To examine the influence of the fractional operator on resultant outcomes, we present the solutions obtained for varying magnitudes of the fractional order α. These are juxtaposed against their precise equivalents derived under the standard condition in which α is equivalent to unity. This has been conducted to ascertain the effects of variable fractional orders, α, and to determine the extent to which alterations in α modify the characteristics of the resultant solutions. The graphical depictions served to elucidate the physical properties of the solutions under investigation. This research demonstrated that the augmented hyperbolic function is an effective analytical instrument for deriving more encompassing exact solutions for numerous NLPDEs relevant to the field of mathematical physics. Future studies could explore the numerical solutions for the FS equation.

Acknowledgment

Compliance with ethical standards

Conflict of interest

The author(s) declared no potential conflicts of interest with respect to the research, authorship, and/or publication of this article.

References

Abdeljawad T and Abd Al-Aziz Ahmed H (2015). On conformable fractional calculus. Journal of Computational and Applied Mathematics, 279: 57-66. https://doi.org/10.1016/j.cam.2014.10.016

Cho GS (1990). Effect of negative ions on stimulated Raman scattering in a plasma. Physics of Fluids B: Plasma Physics, 2(9): 2272-2273. https://doi.org/10.1063/1.859411

El-Ajou A, Al-Zhour Z, Oqielat MA, Momani S, and Hayat T (2019). Series solutions of nonlinear conformable fractional KdV-Burgers equation with some applications. The European Physical Journal Plus, 134: 402. https://doi.org/10.1140/epjp/i2019-12731-x

El-Kalaawy OH (2011). Exact solitary solution of Schamel equation in plasmas with negative ions. Physics of Plasmas, 18: 112302. https://doi.org/10.1063/1.3657422

Ghosh KK, Paul B, Das C, and Paul SN (2008). An analytical study of ion-acoustic solitary waves in a plasma consisting of two-temperature electrons and warm drift ions. Journal of Physics A: Mathematical and Theoretical, 41(33): 335501. https://doi.org/10.1088/1751-8113/41/33/335501

Hafez MG, Talukder MR, and Sakthivel R (2016). Ion acoustic solitary waves in plasmas with nonextensive distributed electrons, positrons and relativistic thermal ions. Indian Journal of Physics, 90: 603-611. https://doi.org/10.1007/s12648-015-0782-9

Hassan MM (2010). New exact solutions of two nonlinear physical models. Communications in Theoretical Physics, 53(4): 596-604. https://doi.org/10.1088/0253-6102/53/4/02

Hietarinta J (1987). A search for bilinear equations passing Hirota's three-soliton condition: II: mKdV-type bilinear equations. Journal of Mathematical Physics, 28(9): 2094-2101. https://doi.org/10.1063/1.527421

Hirota R (2004). The direct method in soliton theory. Cambridge University Press, Cambridge, UK. https://doi.org/10.1017/CBO9780511543043

Karakoç SBG, Ali KK, and Mehanna M (2023). Exact traveling wave solutions of the Schamel-KdV equation with two different methods. Universal Journal of Mathematics and Applications, 6(2): 65-75. https://doi.org/10.32323/ujma.1287524

Khalil R, Al Horani M, Yousef A, and Sababheh M (2014). A new definition of fractional derivative. Journal of Computational and Applied Mathematics, 264: 65-70. https://doi.org/10.1016/j.cam.2014.01.002

Rehman HU, Awan AU, Tag-ElDin EM, Alhazmi SE, Yassen MF, and Haider R (2022). Extended hyperbolic function method for the (2+1)-dimensional nonlinear soliton equation. Results in Physics, 40: 105802. https://doi.org/10.1016/j.rinp.2022.105802

Rezazadeh H, Korkmaz A, Achab AE, Adel W, and Bekir A (2021). New travelling wave solution-based new Riccati equation for solving KdV and modified KdV equations. Applied Mathematics and Nonlinear Sciences, 6(1): 447-458. https://doi.org/10.2478/amns.2020.2.00034

Scales WA and Bernhardt PA (1991). Simulation of high-speed (orbital) releases of electron attachment materials in the ionosphere. Journal of Geophysical Research: Space Physics, 96(A8): 13815-13828. https://doi.org/10.1029/91JA01084

Schamel H (1973). A modified Korteweg-de Vries equation for ion acoustic wavess due to resonant electrons. Journal of Plasma Physics, 9(3): 377-387. https://doi.org/10.1017/S002237780000756X

Shang Y (2008). The extended hyperbolic function method and exact solutions of the long–short wave resonance equations. Chaos, Solitons and Fractals, 36(3): 762-771. https://doi.org/10.1016/j.chaos.2006.07.007

Sirendaoreji (2007). Exact travelling wave solutions for four forms of nonlinear Klein–Gordon equations. Physics Letters A, 363(5-6): 440-447. https://doi.org/10.1016/j.physleta.2006.11.049

Wazwaz AM (2010). Partial differential equations and solitary waves theory. Springer Science and Business Media, Berlin, Germany. https://doi.org/10.1007/978-3-642-00251-9

Williams G, Verheest F, Hellberg MA, Anowar MGM, and Kourakis I (2014). A Schamel equation for ion acoustic waves in superthermal plasmas. Physics of Plasmas, 21: 092103. https://doi.org/10.1063/1.4894115

Xue-Qin Z and Hong-Yan Z (2008). An improved f-expansion method and its application to coupled Drinfel'd–Sokolov–Wilson equation. Communications in Theoretical Physics, 50(2): 309-314. https://doi.org/10.1088/0253-6102/50/2/05

Zhong S, Zhao Z, and Wan X (2023). Solitons for the coupled matrix nonlinear Schrödinger-type equations and the related Schrödinger flow. Open Mathematics, 21: 20220600. https://doi.org/10.1515/math-2022-0600